The Astrophysical Journal Letters, 872:L20 (6pp), 2019 February 20 https://doi.org/10.3847/2041-8213/ab04f0

A Method to Search for Black Hole Candidates with Giant Companions by LAMOST

Wei-Min Gu[1], Hui-Jun Mu[1], Jin-Bo Fu[1], Ling-Lin Zheng[1], Tuan Yi[1], Zhong-Rui Bai[2], Song Wang[2], Hao-Tong Zhang[2], Ya-Juan Lei[2], Yu Bai[2], Jianfeng Wu[1], Junfeng Wang[1], and Jifeng Liu[2,3]
[1] Department of Astronomy, Xiamen University, Xiamen, Fujian 361005, People's Republic of China; guwm@xmu.edu.cn
[2] National Astronomical Observatories, Chinese Academy of Sciences, Beijing 100012, People's Republic of China
[3] College of Astronomy and Space Sciences, University of Chinese Academy of Sciences, Beijing 100049, People's Republic of China
Received 2019 January 9; revised 2019 January 31; accepted 2019 February 6; published 2019 February 19

Abstract

We propose a method to search for stellar-mass black hole (BH) candidates with giant companions from spectroscopic observations. Based on the stellar spectra of Large sky Area Multi-Object fiber Spectroscopic Telescope (LAMOST) Data Release 6, we obtain a sample of seven giants in binaries with large radial velocity variation $\Delta V_R > 80\,\mathrm{km\,s^{-1}}$. With the effective temperature, surface gravity, and metallicity provided by LAMOST, and the parallax given by *Gaia*, we can estimate the mass and radius of the giant, and therefore evaluate the possible mass of the optically invisible star in the binary. We show that the sources in our sample are potential BH candidates, and are worthy of dynamical measurement by further spectroscopic observations. Our method may be particularly valid for the selection of BH candidates in binaries with unknown orbital periods.

Key words: binaries: general – stars: black holes – stars: kinematics and dynamics

1. Introduction

According to the stellar evolution model, there may exist $\sim 10^8$ to 10^9 stellar-mass black holes (BHs) in our Galaxy (e.g., Brown & Bethe 1994; Timmes et al. 1996). However, only around 20 BHs have been dynamically confirmed since the first BH was found in 1972 (Bolton 1972; Webster & Murdin 1972). In addition, there are tens of BH candidates without dynamical identification. In total, the sum of confirmed BHs and candidates is less than one hundred in our Galaxy (Corral-Santana et al. 2016). It is known that most of the confirmed BHs and candidates were originally selected from the X-ray observations. In general, an X-ray burst in a binary means that a neutron star (NS) or a BH may exist in the binary. If the radiation contains no typical characteristics of NS systems, such as the type I X-ray burst or the radio pulses, the compact object can be regarded as a BH candidate. If the follow-up dynamical measurement with spectroscopic observations can derive that the compact object mass is larger than $3\,M_\odot$ (e.g., Casares & Jonker 2014), then a BH is identified. Such a classic method, based on the semi-amplitude of the radial velocity variation K and the orbital period $P_{\rm orb}$ obtained from the radial velocity curve, is well understood but may not be efficient.

The potential to search for BHs or BH candidates according to some surveys has been widely studied. Analysis of *Gaia* data related to this issue (e.g., Breivik et al. 2017; Mashian & Loeb 2017; Yalinewich et al. 2018; Yamaguchi et al. 2018) predicted that hundreds or thousands of BHs may be found by the end of its five-year mission. Masuda & Hotokezaka (2018) discussed the potential of the *Transiting Exoplanet Survey Satellite* to identify and characterize nearby BHs with stellar companions on short-period orbits. By exploring the Optical Gravitational Lensing Experiment in its third generation (OGLE-III) database of 150 million objects, Wyrzykowski et al. (2016) identified 13 microlensing events that are consistent with having compact object lens.

A large number of BHs may exist in binaries, with or without very weak X-ray emission. Thus, different methods are required in order to search for more existent BHs in our Galaxy. For example, some physical parameters for binary systems are well constrained by the spectroscopic observations (e.g., Mazeh & Goldberg 1992; Marsh et al. 1994; Duemmler et al. 1997). The Large sky Area Multi-Object fiber Spectroscopic Telescope (LAMOST; also called Guoshoujing Telescope; Wang et al. 1996; Su & Cui 2004; Cui et al. 2012) survey is a large-scale spectroscopic survey. The large number of LAMOST stellar spectra that have been released enable us to search for BH candidates in a specific way, i.e., without the X-ray bursts and simply from the spectroscopic observations.

The LAMOST Experiment for Galactic Understanding and Exploration survey of Milky Way stellar structure has derived millions of stellar spectra. Around nine million stellar spectra have been released by LAMOST. We can search for BH candidates in binaries based on these spectra. This Letter focuses on the binary system containing a giant star, and is organized as follows. The method is described in Section 2. Our sample and data analyses are shown in Section 3. The sources in our sample are investigated in Section 4. Conclusions and a discussion are presented in Section 5.

2. Method

In a binary system with a compact object, the optically visible star is denoted as M_1, and the compact object is denoted as M_2. For simplicity, a circular orbit is assumed for the binary. Then, a basic dynamical equation takes the form

$$\frac{GM_2}{a^2} = \frac{V_{\rm K}^2}{a_1}, \tag{1}$$

where a is the separation of the binary, and a_1 is the distance between M_1 and the center of mass, with $a_1/a = M_2/(M_1 + M_2)$. $V_{\rm K}$ is the Keplerian velocity of M_1 in the circular orbit. In addition, we introduce a parameter "K" to describe the semi-amplitude of the radial velocity variation during a circle. Thus, $K = V_{\rm K} \sin i$, where i is the inclination angle of the orbital plane.

We define $R_{\rm L1}$ as the effective Roche-lobe radius, which is expressed as (Eggleton 1983)

$$\frac{R_{\rm L1}}{a} = \frac{0.49q^{2/3}}{0.6q^{2/3} + \ln(1 + q^{1/3})} \quad (2)$$

where $q \equiv M_1/M_2$. By combining Equations (1)–(2) we obtain

$$\frac{K^2 R_{\rm L1}}{GM_1 \sin^2 i} = f(q) = \frac{0.49q^{-1/3}(1 + q)^{-1}}{0.6q^{2/3} + \ln(1 + q^{1/3})}. \quad (3)$$

In general, we can assume that $R_1 \leqslant R_{\rm L1}$. If M_1 can just fill its Roche lobe, then we have $R_1 = R_{\rm L1}$. Otherwise, the Roche lobe is not filled out, thus $R_1 < R_{\rm L1}$. In this work, we define $R_1 = \lambda R_{\rm L1}$ $(0 < \lambda \leqslant 1)$. The radius can be expressed as $R_1 = (GM_1/g)^{1/2}$, where g is the surface gravity. Then, Equation (3) can be modified as

$$\frac{K^2}{\lambda \sin^2 i \sqrt{GM_1 g}} = f(q). \quad (4)$$

Obviously, there exists $K \geqslant \Delta V_R/2$, where ΔV_R is the largest variation of the radial velocity among all the spectroscopic observations for a certain source. Thus, Equation (4) implies

$$\frac{\Delta V_R^2}{4\lambda \sin^2 i \sqrt{GM_1 g}} \leqslant f(q). \quad (5)$$

Interestingly, $f(q)$ is a monotonic function, i.e., $f(q)$ always decreases with increasing q. For a given pair of parameters (i, λ), as indicated by the above inequality, with the known values for ΔV_R, $\log g$, and M_1 from spectroscopic observations, the lower limit for $f(q)$ corresponds to an upper limit for q (denoted as $q^{\rm max}$), thus a lower limit for M_2 (denoted as $M_2^{\rm min}$). For a reasonable pair (i, λ), if $M_2^{\rm min} > 3M_\odot$ and $M_2^{\rm min} > M_1$ are both matched (as M_1 is already a giant and therefore $M_2^{\rm min} > M_1$ means that M_2 cannot be a main sequence star), the optically invisible star may be regarded as a potential BH candidate. In particular, for the extreme case with $\sin i = 1$ and $\lambda = 1$, if $M_2^{\rm min} > 3M_\odot$ and $M_2^{\rm min} > M_1$ are both satisfied, then the object M_2 can be regarded as an identified BH.

Here, we would stress that our method is particularly introduced for the case that the orbital period of the binary is unknown. Otherwise, as mentioned in Section 1, M_2 can be estimated by the classic method, which is based on the semi-amplitude K and the orbital period $P_{\rm orb}$.

3. Sample and Analyses

Recently, a huge number of stellar spectra from LAMOST Data Release 6[4] (LDR6), together with the released observations of *Gaia* Data Release 2 (GDR2; Gaia Collaboration et al. 2018), have enabled us to search for BH candidates through a specific way, i.e., simply from the spectroscopic observations. In LDR6, the "A-, F-, G-, and K-type star catalog" (see footnote) provides the important stellar astrophysical parameters, such as the effective temperature $T_{\rm eff}$, the surface gravity $\log g$, the metallicity [Fe/H], and their errors by the LAMOST Stellar Parameter pipeline (LASP; Luo et al. 2015). In addition, the LAMOST 1D pipeline works on the measurement of heliocentric radial velocity (V_R) for stars by using a cross-correlation method (Luo et al. 2015).

Liu et al. (2015) selected the metal-rich giant stars with $3500 < T_{\rm eff} < 6000$ K, $\log g < 4.0$ dex, and [Fe/H] > -0.6 dex. In this Letter, the giant stars are selected by containing repeated radial velocity measurements (at least three times) in LDR6 within 3″, and match the following selection criteria.

(i) The signal-to-noise ratio (S/N) S/N > 10 is required in the g-[5] and r-bands.[6]
(ii) Our main focus is the G and K giant stars. Thus, the surface gravity $\log g < 3.0$ dex and the effective temperature 3500 K $< T_{\rm eff} <$ 6000 K are adopted.
(iii) The stellar spectra have only shifted single-line (without double peaks) with a large variation of radial velocity, $\Delta V_R > 80$ km s^{-1}.[7]

Our sample consists of seven binaries, each of which has a giant star. The observational data of our sample are shown in Table 1.

4. BH Candidates

Following the method described in Section 2, with a given pair of parameters (i, λ) and the known values of ΔV_R and $\log g$ from LAMOST spectra, we can study the possibility of BH candidates in our sample. A comparison of the observations with the theory in the $\Delta V_R/2 - \log g$ diagram is shown in Figure 1. For the theoretical results, we choose the well-known critical mass $M_2 = 3M_\odot$ for the optically invisible star, and two typical mass $M_1 = 1M_\odot$ and $2\,M_\odot$ for the observed giant star. As indicated by Inequality (5), for a given $\log g$, there is an upper limit for $\Delta V_R/2$. If the observational $\Delta V_R/2$ is larger than the theoretical maximal value, then a larger mass than $3\,M_\odot$ is required for M_2. In such a case, the source is likely to be a BH candidate. Here, we adopt the extreme case ($i = 90°$) and a typical case ($i = 60°$) for the inclination angle. In addition, for the radius ratio $\lambda = R_1/R_{\rm L1}$, we take the extreme case ($\lambda = 1$) and two reasonable cases $\lambda = 0.5$ and 0.2[8] for the analysis. The theoretical results for $M_1 = 1\,M_\odot$ and $2\,M_\odot$ are, respectively, shown by the solid and dashed lines, where the red, green, and black lines correspond to "$i = 90°$, $\lambda = 1$," "$i = 60°$, $\lambda = 0.5$," and "$i = 60°$, $\lambda = 0.2$," respectively.

All seven sources in our sample are also plotted in this diagram by the blue circles. Figure 1 illustrates that there is no source above the red dashed or solid line, which means that none of these sources can be regarded as an identified BH according to the current spectroscopic observations. All of the sources are located between the green solid line and the black dashed line, which indicates that, for reasonable parameters such as $i \sim 60°$ and $\lambda \sim 0.2$–0.5, the optically invisible star is likely to be a BH candidate. Moreover, because the observational $\Delta V_R/2$ is only a lower limit for the real K, the latter may

[4] http://dr6.lamost.org/

[5] We use the S/N at the g-band because most of the spectral lines sensitive to $\log g$ are located in the range of wavelength (~4000–5300 Å; Liu et al. 2014, 2015).

[6] The radial velocity from LAMOST is mainly from the lines in ~4000–6600 Å.

[7] According to Inequality (5), a larger ΔV_R corresponds to a higher $M_2^{\rm min}$, so we choose a relatively large velocity (80 km s^{-1}) as a lower limit, beyond which there is a sample of several sources for detailed investigation.

[8] As some prediction shows, e.g., Figure 1 of Mashian & Loeb (2017), a large fraction of BH binaries have quite long orbital periods (~years), where the radius of the optically observed star can be far below the corresponding Roche-lobe radius. Thus, the values of 0.5 and 0.2 for λ are reasonable.

Table 1
Parameters for the Sources in Our Sample

No.	R.A.	Decl.	UCAC4	Vmag (mag)	$T_{\rm eff}$ (K)	$\log g$ (dex)	[Fe/H] (dex)	$N_{\rm obs}$	ΔV_R (km s^{-1})	ϖ (mas)	$R_{\rm l}^{\rm G}$ ($R_\odot$)	$R_{\rm l}^{\rm LT}$ ($R_\odot$)
(1)	(2)	(3)	(4)	(5)	(6)	(7)	(8)	(9)	(10)	(11)	(12)	(13)
1	0.839246	38.518578	643–000232	12.736 ± 0.05	4696 ± 36	2.65 ± 0.06	−0.25 ± 0.03	3	93.5 ± 5.6	0.505 ± 0.043	9.15	10.8 ± 0.2
2	3.887134	38.688854	644–000944	12.665 ± 0.09	4301 ± 22	1.95 ± 0.04	−0.47 ± 0.02	4	83.7 ± 6.2	0.379 ± 0.032	15.82	19.7 ± 0.3
3	58.561194	45.43539	678–024276	15.054 ± 0.03	4943 ± 108	2.48 ± 0.17	−0.65 ± 0.10	3	81.9 ± 9.0	0.148 ± 0.034	⋯	14.7 ± 0.7
4	74.0532211	54.0059047	721–037069	12.784 ± 0.11	4823 ± 53	2.74 ± 0.08	−0.29 ± 0.05	4	107.5 ± 7.4	1.068 ± 0.034	6.34	7.0 ± 0.2
5	106.45855	13.606334	519–037128	14.51 ± 0.02	4655 ± 21	2.53 ± 0.03	−0.31 ± 0.02	3	87.5 ± 5.3	0.122 ± 0.030	⋯	18.4 ± 0.2
6	111.33637	28.067468	591–041200	14.698 ± 0.07	4832 ± 83	2.73 ± 0.13	−0.23 ± 0.08	6	85.1 ± 7.6	0.152 ± 0.032	⋯	11.9 ± 0.4
7	169.1288227	55.7284139	729–048720	10.638 ± 0.17	4191 ± 80	1.82 ± 0.12	−0.75 ± 0.07	3	97.8 ± 5.8	1.086 ± 0.031	13.14	17.9 ± 0.7

Note. Column (1): number of the source. Column (2): R.A. (J2000). Column (3): decl. (J2000). Column (4): UCAC4 recommended identifier. Column (5): *V*-band magnitude from UCAC4. Column (6): effective temperature from LDR6. Column (7): surface gravity from LDR6. Column (8): metallicity from LDR6. Column (9): times of observations. Column (10): observed largest variation of radial velocity. Column (11): absolute stellar parallax from GDR2. Column (12): radius of the giant star from GDR2. Column (13): radius of the giant star based on the relation of the bolometric luminosity and the effective temperature.

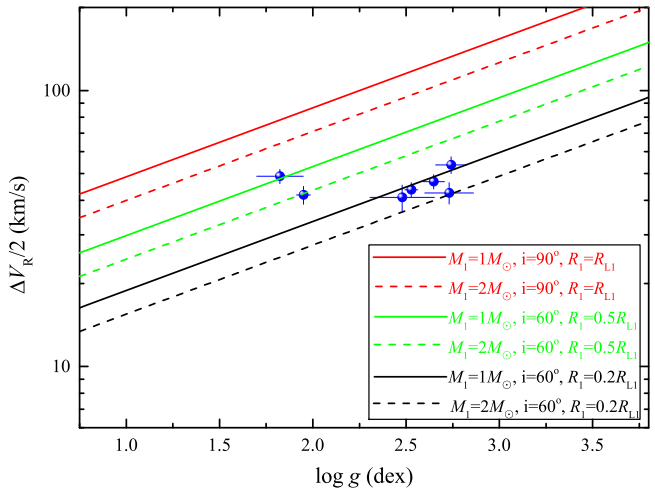

Figure 1. Comparison of the observations (blue circles) with the theoretical results (lines) in the $\Delta V_R/2 - \log g$ diagram, where $M_2 = 3\,M_\odot$ is adopted for the theoretical calculations.

be significantly larger than the former, particularly for the sources with only three times of observations. If the physical parameter of the vertical axis in Figure 1 is replaced by the real K, the location of the seven sources should be moved upward. Thus, more spectroscopic observations are required to make a judgment.

In addition, we check the seven sources in our sample to be real giant stars through a different way, i.e., without using the values of $\log g$ from LAMOST. The radius can be estimated by the relation $L_{\rm bol} = 4\pi R_1^2 \sigma T_{\rm eff}^4$, where $L_{\rm bol}$ is the bolometric luminosity of the giant star, and $T_{\rm eff}$ is given by LDR6. In order to obtain the proper $L_{\rm bol}$, we should take the extinction into account. The reddening $E(B-V)$ is referred to the Pan-STARRS 3D Dust Map (Green et al. 2018). The interstellar extinction A_V is calculated by using the Fitzpatrick reddening law: $R_V = 3.1$ (Fitzpatrick 1999). Then $L_{\rm bol}$ is calculated by the following: (a) parallax given by *Gaia*; (b) V-band magnitude from UCAC4 (Zacharias et al. 2012), as shown in columns 4 and 5 of Table 1; (c) extinction A_V; (d) bolometric correction as a function of $T_{\rm eff}$ (Torres 2010). The derived radius $R_1^{\rm LT}$ is shown in Table 1, where the superscript "LT" means that the radius is based on the bolometric luminosity $L_{\rm bol}$ and the effective temperature $T_{\rm eff}$. Moreover, GDR2 provides the radius $R_1^{\rm G}$ for some sources in our sample, which is also shown in Table 1. It is seen by $R_1^{\rm LT}$ and $R_1^{\rm G}$ that the sources in our sample are real giant stars with $R_1 \gg R_\odot$.

In order to evaluate the mass for the optically invisible star in the binary, we first obtain a more convincing pair of (M_1, R_1) through the PARSEC model,[9] by given $T_{\rm eff}$, $\log g$, and [Fe/H] from LAMOST. The obtained stellar parameters (the age, R_1, and M_1) are presented in Table 2, which shows that M_1 is in the range $1 \sim 2\,M_\odot$. That is why we choose $M_1 = 1\,M_\odot$ and $2\,M_\odot$ for the theoretical analyses in Figure 1.

Based on the obtained M_1 and R_1 in Table 2, and the given pair of parameters (i, λ), together with the simple assumption $K = \Delta V_R/2$, we can derive the mass M_2 by solving the following equation:

$$\frac{\Delta V_R^2 \cdot R_1}{4\lambda G M_1 \sin^2 i} = f(q), \tag{6}$$

where the above equation is slightly transformed from Equation (3). The results of our evaluation of M_2 for the seven sources in our sample are shown in Table 2 and Figure 2,[10] where three pairs of (i, λ) are adopted. For sources No. 2 and No. 7, as shown in Table 2, $M_1 = 0.9\,M_\odot$ itself is the lower bound according to the PARSEC model, below which the lifetime of the main sequence stage is around or even exceeds the age of the universe. Thus, arrows are used instead of error bars in Figure 2 for these two sources. It is seen from Figure 2 that, for the extreme case, "$i = 90°$ and $\lambda = 1$," the mass M_2 is below the critical mass $M_2 = 3\,M_\odot$, which agrees with the results in Figure 1. Thus, there is no identified BH in our sample according to the current observations. However, for some reasonable parameters "$i = 60°$ and $\lambda = 0.5$ or 0.2," Figure 2 shows that the sources can approach or even go beyond the critical blue dashed line, which indicates that $M_2 > 3\,M_\odot$ can be matched. In addition, because $M_1 \lesssim 2\,M_\odot$ exists for our sample, $M_2 > 3\,M_\odot$ means that $M_2 > M_1$ is simultaneously matched. In such case, the optically invisible star is likely to be a BH candidate. In our opinion, with regard to the observed large radial velocity variation and the large radius of M_1, all of the sources in our sample have the potential to be BH candidates, and they are worthy of further dynamical measurement.

Moreover, we check whether or not the sources in our sample have been studied in published catalogs. We cross-match our sources with the radio and X-ray catalogs using a matching radius of 10″. No corresponding radio source was found according to the FIRST CATALOG and the 1.4 GHz NRAO VLA Sky Survey (NVSS). Only one source (No. 4) was known as a faint X-ray source according to the *ROSAT* observations (4.38″ of the distance to the center; Voges et al. 2000).[11] Thus, source No. 4 is likely a BH or an NS system with mass transfer from the giant to the compact object. Furthermore, source No. 7 has measurements by Tycho-2 (Høg et al. 2000).

5. Conclusions and Discussion

In this Letter we have proposed a method, from spectroscopic observations by LAMOST, to search for stellar-mass BH candidates with giant companions. Based on the spectra of LDR6, we have derived a sample of seven giants in binaries with large radial velocity variation $\Delta V_R > 80\,{\rm km\,s^{-1}}$. With $T_{\rm eff}$, $\log g$, and [Fe/H] provided by LAMOST and the parallax given by *Gaia*, we can estimate the values for M_1 and R_1. Moreover, we have evaluated the possible mass of M_2 for the extreme case $i = 90°$ and a typical case $i = 60°$, and the extreme case $\lambda = 1$ and two reasonable cases $\lambda = 0.5$ and 0.2. We argue that the sources in our sample are potential BH

[9] See the PARSEC model http://stev.oapd.inaf.it/cgi-bin/cmd_3.1 for details.

[10] As shown in Table 2, two sources (No. 1 and No. 5) have the same value for M_1, and have the same value for M_2 for a given pair (i, λ), so that the corresponding two circles should be located at the same position for each color. Here, we plot with the derived values without restriction to two significant digits, so that the two circles can be distinguished.

[11] We use HEASARC Browse to cross-match our sources with the *Chandra*, *XMM-Newton*, *Swift*, and *ROSAT* observations.

Table 2
Evaluation of M_2 for the Sources in Our Sample

No.	Age (10^9 yr)	M_1 ($M_\odot$)	R_1 ($R_\odot$)	$M_2^{\rm I}$ ($M_\odot$)	$M_2^{\rm II}$ ($M_\odot$)	$M_2^{\rm III}$ ($M_\odot$)
(1)	(2)	(3)	(4)	(5)	(6)	(7)
1	$7.3^{+4.7}_{-3.8}$	$1.1^{+0.3}_{-0.1}$	$8.1^{+1.5}_{-0.8}$	0.6 ± 0.1	1.3 ± 0.3	2.9 ± 0.8
2†	$13^{+2.2}_{-0.1}$	$0.9^{+1.5}_{-}$	$17.8^{+0.6}_{-}$	$0.9^{+0.4}_{-}$	$2.0^{+0.7}_{-}$	$5.3^{+0.7}_{-}$
3	$0.97^{+9.64}_{-0.33}$	$2.0^{+0.4}_{-1.1}$	$13.3^{+2.7}_{-3.7}$	0.9 ± 0.5	1.7 ± 1.0	3.7 ± 2.3
4	$3.2^{+7.6}_{-1.9}$	$1.4^{+0.5}_{-0.4}$	$8.2^{+2.2}_{-1.7}$	0.8 ± 0.3	1.7 ± 0.6	3.8 ± 1.6
5	$6.3^{+3.1}_{-1.9}$	$1.1^{+0.1}_{-0.1}$	$9.5^{+0.8}_{-0.6}$	0.6 ± 0.1	1.3 ± 0.2	2.9 ± 0.6
6	$2.6^{+4.4}_{-1.6}$	$1.5^{+0.6}_{-0.4}$	$8.7^{+2.8}_{-1.9}$	0.6 ± 0.2	1.2 ± 0.5	2.6 ± 1.1
7†	11^{+1}_{-9}	$0.9^{+0.5}_{-}$	$20.8^{+8.1}_{-}$	$1.3^{+0.7}_{-}$	$3.2^{+1.8}_{-}$	$9.3^{+5.2}_{-}$

Note. † The parameters of the second and the seventh sources cannot be well constrained, where $M_1 = 0.9\,M_\odot$ itself is the lower bound according to the PARSEC model. Column (1): number of the source. Column (2): age of the giant star from the PARSEC model. Column (3): mass of the giant star from the PARSEC model. Column (4): radius of the giant star from the PARSEC model. All the errors about the PARSEC model are 90% confidence. Column (5): mass of M_2 for "$i = 90°$, $\lambda = 1$." Column (6): mass of M_2 for "$i = 60°$, $\lambda = 0.5$." Column (7): mass of M_2 for "$i = 60°$, $\lambda = 0.2$."

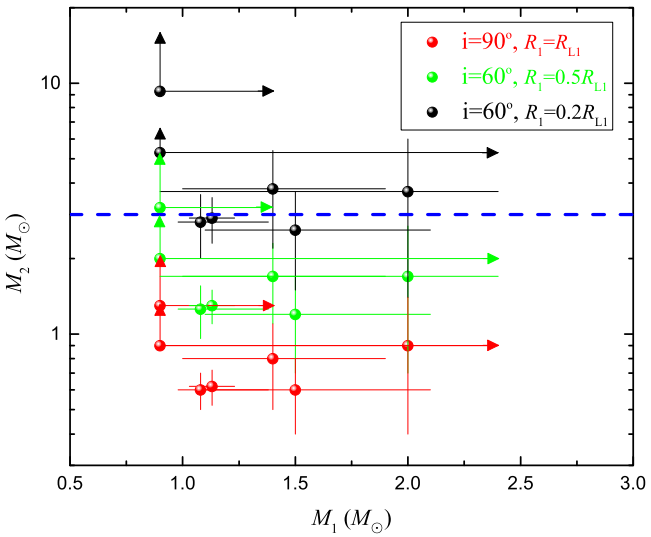

Figure 2. Evaluation of M_2 for the seven sources in our sample based on Equation (6), where three pairs of (i, λ) are adopted. The blue dashed line represents the critical mass $M_2 = 3\,M_\odot$.

candidates and worthy of further dynamical measurement. Our method may be particularly valid to search for BH candidates in binaries with unknown orbital periods.

Our analyses are based on the circular orbit assumption. However, the binary system may have an elliptical orbit (the eccentricity $e \neq 0$). Moe & Di Stefano (2017) investigated the relationship between the orbital period and the eccentricity for early-type binaries identified by spectroscopy, which showed that binaries have small eccentricities $e \lesssim 0.4$ for relatively short orbital periods ($P_{\rm orb} \lesssim 20$ days). On the other hand, for intermediate and long periods, the range of eccentricity can be much wider, as shown by their Equation (3) and Figure (6). In the cases with eccentricity, we can assume that the Roche-lobe radius at the pericenter should not be less than R_1 (otherwise, if the optically invisible star is an NS or a BH, strong X-ray radiation can be produced when the giant star passes through the pericenter). Thus, for a given $R_{\rm L1}$, the lower limit for the separation a (major axis of the elliptical orbit) should be enhanced for $e > 0$, and therefore the lower limit $M_2^{\rm min}$ will be even larger. For a rough estimate, we have the following analytic inequality instead of Inequality (5) in Section 2:

$$\frac{\Delta V_R^2 (1+e)}{4\lambda \sin^2 i \sqrt{G M_1 g}} \leqslant f(q), \tag{7}$$

which implies an even larger $M_2^{\rm min}$ than the case with $e = 0$. Thus, our analyses based on the circular orbit assumption are reliable, in particular for the analytic lower mass limit for M_2.

The possibility of identifying BHs in detached binaries has been discussed for decades (Guseinov & Zel'dovich 1966; Trimble & Thorne 1969), where a method was provided based on single-line spectroscopic binaries with large radial velocity variations. With such a method, a BH candidate has recently been discovered with an orbital period of 83 days (Thompson et al. 2018). We should stress the difference between their method and ours. In their method, the orbital period is a necessary condition for the calculation. On the contrary, our method is based on the comparison of R_1 with the Roche-lobe radius $R_{\rm L1}$, whereas the orbital period is unknown, as discussed in the last paragraph of Section 2. In addition, based on near-infrared observations with the VISTA Variables in the Vía Láctea Survey (VVV), a microlensing stellar-mass BH candidate was discovered, which is likely a good isolated BH candidate (Minniti et al. 2015). Moreover, Giesers et al. (2018) found a detached stellar-mass BH candidate in the globular cluster NGC 3201 by performing multiple epoch spectroscopic observations.

Furthermore, we can expect that, with growing data released by LAMOST, particularly for the ongoing LAMOST Medium Resolution Survey, the proposed method in the present work may be helpful to select a large number of BH candidates with giant companions. Moreover, our method can be directly applied to the SDSS APOGEE data to search for BH candidates, which provide high-resolution spectra on giant stars.

We thank Yi-Ze Dong, Fan Yang, and Mou-Yuan Sun for beneficial discussions, and thank the referee for helpful suggestions that improved the manuscript. This work was supported by the National Natural Science Foundation of China (NSFC) under grants 11573023, 11603035, U1831205, 11425313, and 11333004. Guoshoujing Telescope (the Large Sky Area Multi-Object Fiber Spectroscopic Telescope, LAMOST) is a National Major Scientific Project built by the

Chinese Academy of Sciences. Funding for the project has been provided by the National Development and Reform Commission. LAMOST is operated and managed by the National Astronomical Observatories, Chinese Academy of Sciences.

ORCID iDs

Wei-Min Gu https://orcid.org/0000-0003-3137-1851
Hui-Jun Mu https://orcid.org/0000-0001-6589-2220
Song Wang https://orcid.org/0000-0003-3116-5038
Yu Bai https://orcid.org/0000-0002-4740-3857
Jianfeng Wu https://orcid.org/0000-0001-7349-4695
Junfeng Wang https://orcid.org/0000-0003-4874-0369

References

Bolton, C. T. 1972, Natur, 235, 271
Breivik, K., Chatterjee, S., & Larson, S. L. 2017, ApJL, 850, L13
Brown, G. E., & Bethe, H. A. 1994, ApJ, 423, 659
Casares, J., & Jonker, P. G. 2014, SSRv, 183, 223
Corral-Santana, J. M., Casares, J., Muñoz-Darias, T., et al. 2016, A&A, 587, A61
Cui, X.-Q., Zhao, Y.-H., Chu, Y.-Q., et al. 2012, RAA, 12, 1197
Duemmler, R., Ilyin, I. V., & Tuominen, I. 1997, A&AS, 123, 209
Eggleton, P. P. 1983, ApJ, 268, 368
Fitzpatrick, E. L. 1999, PASP, 111, 63
Gaia Collaboration, Brown, A. G. A., Vallenari, A., et al. 2018, A&A, 616, A1
Giesers, B., Dreizler, S., Husser, T.-O., et al. 2018, MNRAS, 475, L15
Green, G. M., Schlafly, E. F., Finkbeiner, D., et al. 2018, MNRAS, 478, 651
Guseinov, O. K., & Zel'dovich, Y. B. 1966, SvA, 10, 251
Høg, E., Fabricius, C., Makarov, V. V., et al. 2000, A&A, 355, L27
Liu, C., Deng, L.-C., Carlin, J. L., et al. 2014, ApJ, 790, 110
Liu, C., Fang, M., Wu, Y., et al. 2015, ApJ, 807, 4
Luo, A.-L., Zhao, Y.-H., Zhao, G., et al. 2015, RAA, 15, 1095
Marsh, T. R., Robinson, E. L., & Wood, J. H. 1994, MNRAS, 266, 137
Mashian, N., & Loeb, A. 2017, MNRAS, 470, 2611
Masuda, K., & Hotokezaka, K. 2018, arXiv:1808.10856
Mazeh, T., & Goldberg, D. 1992, ApJ, 394, 592
Minniti, D., Contreras Ramos, R., Alonso-García, J., et al. 2015, ApJL, 810, L20
Moe, M., & Di Stefano, R. 2017, ApJS, 230, 15
Su, D.-Q., & Cui, X.-Q. 2004, ChJAA, 4, 1
Thompson, T. A., Kochanek, C. S., Stanek, K. Z., et al. 2018, arXiv:1806.02751
Timmes, F. X., Woosley, S. E., & Weaver, T. A. 1996, ApJ, 457, 834
Torres, G. 2010, AJ, 140, 1158
Trimble, V. L., & Thorne, K. S. 1969, ApJ, 156, 1013
Voges, W., Aschenbach, B., Boller, T., et al. 2000, IAUC, 7432, 1
Wang, S.-G., Su, D.-Q., Chu, Y.-Q., Cui, X., & Wang, Y.-N. 1996, ApOpt, 35, 5155
Webster, B. L., & Murdin, P. 1972, Natur, 235, 37
Wyrzykowski, L., Kostrzewa-Rutkowska, Z., Skowron, J., et al. 2016, MNRAS, 458, 3012
Yalinewich, A., Beniamini, P., Hotokezaka, K., & Zhu, W. 2018, MNRAS, 481, 930
Yamaguchi, M. S., Kawanaka, N., Bulik, T., & Piran, T. 2018, ApJ, 861, 21
Zacharias, N., Finch, C. T., Girard, T. M., et al. 2012, yCat, 1322